Microfield distributions in a classical two-component plasma

2006 J. Phys. A: Math. Gen. 39 4677

(http://iopscience.iop.org/0305-4470/39/17/S56)

INSTITUTE OF PHYSICS PUBLISHING JOURNAL OF PHYSICS A: MATHEMATICAL AND GENERAL

J. Phys. A: Math. Gen. **39** (2006) 4677–4681 doi:10.1088/0305-4470/39/17/S56

Microfield distributions in a classical two-component plasma

H B Nersisyan and G Zwicknagel

Institut für Theoretische Physik, Universität Erlangen, Staudtstr. 7, D-91058 Erlangen, Germany

E-mail: zwicknagel@theorie2.physik.uni-erlangen.de

Received 16 September 2005, in final form 13 December 2005
Published 7 April 2006
Online at stacks.iop.org/JPhysA/39/4677

Abstract
The electric microfield distributions (MFD) at charged and neutral particles in classical electron–ion two-component plasmas are described by a theoretical model based on the exponential and the potential-of-mean-force approximations. The MFDs provided by this theoretical treatment are in good agreement with results from molecular dynamics simulations.

PACS numbers: 52.27.Gr, 52.27.Aj, 52.65.Yy, 05.10.−a

1. Introduction and definitions

Because of the Stark effect the fluctuating electric microfields created by the charged particles in a plasma affect the profiles of spectral lines of atoms and ions immersed in a plasma, and a comparison of experimental and theoretical widths and shapes of spectral lines is a widely used tool for plasma diagnostics [1, 2]. Under certain assumptions [1, 2], the observed spectral line shapes can be closely related to the electric microfield distribution at the radiating atom or ion (radiator) [3]. Within the quasistatic approximation the problem is then reduced to a determination of the probability distribution of the perturbing fields. Until now most work was done here on one-component plasmas (OCP) [4–6], in particular in framework of the very successful adjustable parameter exponential approximation (APEX) scheme [7, 8]. Only a few investigations exist, however, for systems with attractive interactions, as e.g. for a single highly charged impurity ion immersed in an electronic OCP [9] or for genuine two-component plasmas (TCP) [10–12].

Following [12], we consider the electric field $\mathbf{E} = \varepsilon$ at a positive probe charge $Z_R e$ located at $\mathbf{r_0}$ and embedded in a classical TCP of N_i ions and N_e electrons in thermodynamic equilibrium at a temperature T. The average densities of the ions and electrons are n_i and n_e, respectively ($n = n_e + n_i$). The probability of measuring a certain ε is the normalized electric microfield distribution (MFD). Within the classical canonical ensemble it can be represented as

$$Q(\varepsilon) = \langle \delta(\varepsilon - \mathbf{E}) \rangle = \int \frac{\mathrm{e}^{-U(\mathcal{T}_e,\mathcal{T}_i,\mathbf{r}_0)/k_BT}}{W} \delta(\varepsilon - \mathbf{E}(\mathcal{T}_e, \mathcal{T}_i, \mathbf{r}_0))\, \mathrm{d}\mathbf{r}_0\, \mathrm{d}\mathcal{T}_e\, \mathrm{d}\mathcal{T}_i, \tag{1}$$

where $\mathcal{T}_e = \{\mathbf{r}_1, \ldots, \mathbf{r}_{N_e}\}$, $\mathcal{T}_i = \{\mathbf{R}_1, \ldots, \mathbf{R}_{N_i}\}$ are the coordinates of electrons and ions, respectively. Here W is the canonical partition function and $U(\mathcal{T}_e, \mathcal{T}_i, \mathbf{r}_0)$ is the potential energy of the system

$$U(\mathcal{T}_e, \mathcal{T}_i, \mathbf{r}_0) = \frac{1}{2} \sum_{\alpha,\beta} \frac{q_\alpha q_\beta}{4\pi\varepsilon_0} \sum_{a,b} u_{\alpha\beta}(|\mathbf{r}_{a,\alpha} - \mathbf{r}_{b,\beta}|) + \sum_{\alpha,a} \frac{q_\alpha Z_R e}{4\pi\varepsilon_0} u_{\alpha R}(|\mathbf{r}_{a,\alpha} - \mathbf{r}_0|) \tag{2}$$

with $\alpha, \beta = e, i$, $q_{e,i} = -e, Z_i e$, and $\mathbf{r}_{a,e} = \mathbf{r}_a$, $\mathbf{r}_{a,i} = \mathbf{R}_a$. In the first term of equation (2) the sum is restricted to $a \neq b$ for identical particles. The pair interaction potentials are given by the Coulomb potential for repulsive interaction and a regularized interaction in the case of attractive interaction, i.e. $u_{\alpha\alpha}(r) = u_{iR}(r) = 1/r$, $u_{ei}(r) = u_{eR}(r) = (1 - \mathrm{e}^{-r/\delta})/r$. By the regularization quantum diffraction effects at small distances $r \lesssim \delta$ are taken into account [13].

The total electrical field $\mathbf{E}$ at $\mathbf{r}_0$ is a superposition of electronic and ionic single-particle fields and is related to the total potential energy U through $\mathbf{E} = -\nabla_{\mathbf{r}_0} U \big/ Z_R e$. Assuming an isotropic system equation (1) can be rewritten in terms of the distribution function $P(\varepsilon)$ with $P(\varepsilon)\, \mathrm{d}\varepsilon = 4\pi\varepsilon^2 Q(\varepsilon)\, \mathrm{d}\varepsilon$ and the function $T(\mathbf{K})$ as

$$P(\varepsilon) = \frac{2\varepsilon}{\pi} \int_0^\infty T(K) \sin(K\varepsilon) K\, \mathrm{d}K, \qquad T(\mathbf{K}) = \int Q(\varepsilon)\, \mathrm{e}^{\mathrm{i}\mathbf{K}\cdot\varepsilon}\, \mathrm{d}\varepsilon = \langle \mathrm{e}^{\mathrm{i}\mathbf{K}\cdot\mathbf{E}} \rangle. \tag{3}$$

2. Expressing the MFD through pair correlation functions

Following the parameter integration technique used for calculating the MFD in an OCP and employing the 'exponential approximation' ansatz (see [6–9] and references therein) the function $T(K)$, equation (3), can be expressed through the pair correlation functions (PCF) $g_{\alpha R}(r)$ between radiator and plasma particles (see [12] for details):

$$T(K) = \exp\left[-4\pi \sum_\alpha n_\alpha \int_0^\infty \frac{E_\alpha(r)}{\mathcal{E}_\alpha(r)} \left(1 - \frac{\sin(K\mathcal{E}_\alpha(r))}{K\mathcal{E}_\alpha(r)} \right) g_{\alpha R}(r) r^2\, \mathrm{d}r \right]. \tag{4}$$

Here $\mathbf{E}_\alpha(\mathbf{r}) = -(q_\alpha/4\pi\varepsilon_0)\nabla_\mathbf{r} u_{\alpha R}(r)$ and $\boldsymbol{\mathcal{E}}_\alpha(\mathbf{r})$ are the single-particle and effective fields [12], respectively. Expanding $T(K)$ for small K provides the second moment $\langle \varepsilon^2 \rangle = \left\langle (\nabla_{\mathbf{r}_0} U)^2 \right\rangle \big/ (Z_R e)^2$ of the microfield distribution through $T(K) = 1 - \langle \varepsilon^2 \rangle K^2/6 + \cdots$, cf equation (3). The second moment can also be expressed by the $g_{\alpha R}(r)$ and the interactions $u_{\alpha R}(r)$ [12]. This imposes certain conditions on the choice of $\mathcal{E}_\alpha(\mathbf{r})$.

2.1. The PMFEX approximation for the MFD at a charged point

For a OCP very good agreement has been achieved using the APEX [7]. There $\mathcal{E}_\alpha(r)$ is given by the ad hoc ansatz of a Debye field $\mathcal{E}_\alpha(r) \propto (1 + \gamma r)\exp(-\gamma r)/r^2$ where γ is chosen to satisfy the second moment. There exists, however, no straightforward extension of the APEX scheme to a TCP. Instead we successfully applied the potential-of-mean-force (PMF) approximation proposed by Yan and Ichimaru [10],

$$\mathcal{E}_\alpha(r) = \frac{k_B T}{Z_R e} \frac{\partial}{\partial r} [\ln g_{\alpha R}(r)], \tag{5}$$

to the classical TCP at hand. The PMF ansatz (5) automatically satisfies the exact second moment and constitutes together with the exponential approximation (4) the PMFEX approximation where the MFD $P(\varepsilon)$ is entirely expressed by the $g_{\alpha R}$.

2.2. The MFD at a neutral point

The MFD for a charged radiator was already discussed in detail in [12]. Here we are aiming at an extension to the case of a neutral radiator and will provide new analytical and simulation results devoted to this issue. For a neutral radiator, i.e., in the limit $Z_R \to 0$, the PMF ansatz (5) is not applicable, as in this case the PCFs tend to unity, $g_{\alpha R} \to 1$, and $\ln g_{\alpha R}(r) \to 0$. Based on the derivations given in [12] the correct limit $Z_R \to 0$ can, however, be done and results in the effective fields

$$\mathcal{E}_\alpha(r) = E_\alpha(r) \left\{ 1 + \frac{4\pi}{q_\alpha} \sum_\beta q_\beta n_\beta \int_0^r [g_{\alpha\beta}(\rho) - 1]\rho^2 \, \mathrm{d}\rho \right\}, \tag{6}$$

which we use for calculating the MFD at a neutral radiator. Here the single particle fields $E_\alpha(r)$ are the bare Coulomb field of a charge q_α.

3. Numerical treatment and results

In the following the probe charge is either a neutral particle ($Z_R = 0$) or one of the plasma ions ($Z_R = Z_i$). The related classical TCP defined by equation (2) is, for a given Z_i and $n_i = n_e/Z_i$, completely determined by the potential parameter δ and the classical plasma parameter $\Gamma_{ee} = (e^2/4\pi\varepsilon_0 k_B T)(4\pi n_e/3)^{1/3}$. The required $g_{\alpha R}$ are calculated by solving numerically the hyper-netted-chain (HNC) integral equations for these systems. The MFD $P(\varepsilon)$ is then calculated via equations (3), (4) and (5) or (6). For comparison we also sampled the corresponding MFD from molecular dynamics (MD) simulations of the classical TCPs at hand and $N_i + N_e = 2002$ particles. For more details on the numerical treatment and the MD simulations, see [12].

Such HNC and MD calculations have been done for various Z_i, Γ_{ee} and δ. Some examples for the resulting MFD are given in figures 1 and 2 for the cases of H^+ ($n_e = n_i$) and Al^{13+} ($n_e = 13n_i$) TCPs. The electrical field E is scaled throughout in units of the Holtsmark field for a TCP $E_H = e(8\pi/25)^{1/3}\left[Z_i\left(1 + Z_i^{1/2}\right)/(Z_i + 1)\right]^{2/3}/4\pi\varepsilon_0 a^2$ where $a = (4\pi n/3)^{-1/3}$. Both for a charged ($Z_R = Z_i$) and a neutral ($Z_R = 0$) radiator the MFD of the correlated systems clearly deviates from the Holtsmark distribution for an uncorrelated TCP (i.e. $\Gamma_{ee} \to 0$) towards lower field strength (see figure 1). Comparing neutral and charged points, interesting differences in the location of the maximum of the MFD show up. In the highly charged Al^{13+} plasma it shifts towards higher values and slightly lower field strength when going from the neutral to the charged reference point, in agreement with earlier observations made for the MFD of a OCP (e.g. in [5]). This can be ascribed to the strong ion–ion repulsion, which here prevails over the electronic contribution. For hydrogen at the given parameters the maximum, however, shifts in the opposite way. Here the electronic contribution obviously increases the total field at the charged point compared to a neutral point.

For charged radiators $Z_R = Z_i$ (upper part of figure 1) the PMFEX approach (equations (3), (4), (5)) very well agrees with the simulation data except of cases with rather large coupling like the example of a H^+ plasma with $\Gamma_{ee} = 1.0$. Here some deviations show up. A similar good agreement of the analytical treatment with the MD data can be achieved as well for a neutral radiator (lower part of figure 1) by using in expression (4) the effective

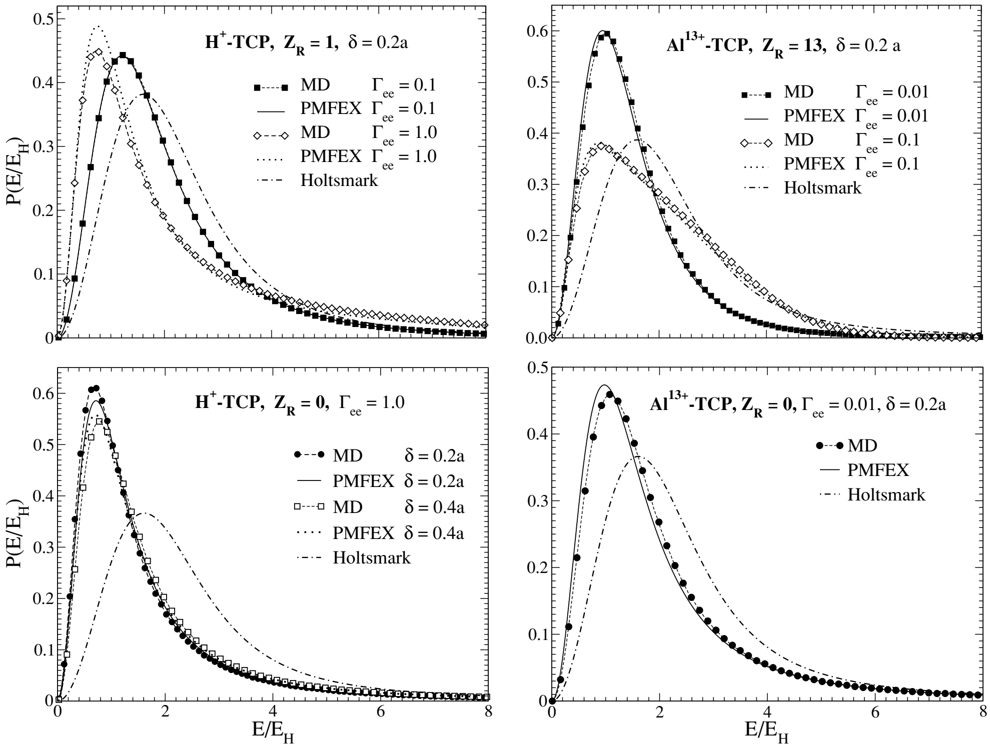

Figure 1. Normalized MFD for hydrogen (left panel) and Al^{13+} (right panel) plasmas at a charged (top) and a neutral (bottom) radiator for different δ and Γ_{ee} obtained form MD simulations and the PMFEX treatment as indicated. For comparison the Holtsmark distribution (see [12]) is also shown.

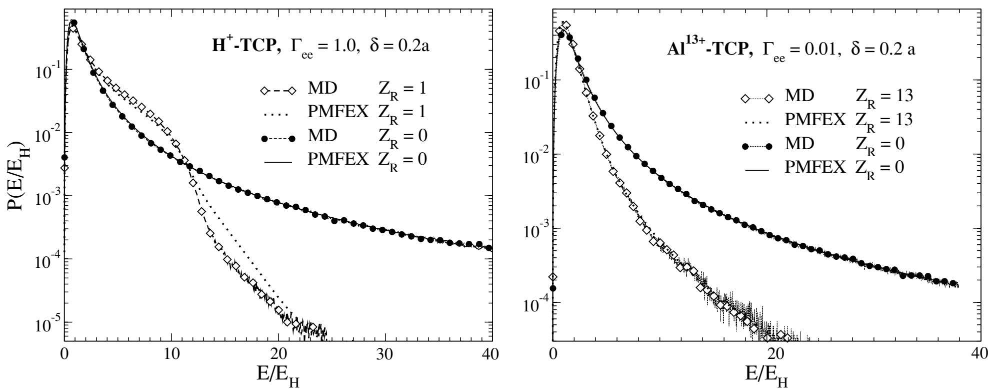

Figure 2. Behaviour of the normalized MFD at large field strengths for some selected cases of figure 1.

fields as given through equation (6). The PMFEX approach also predicts very well the high field behaviour of the MFD (see figure 2) which shows a quite different decay for $Z_R = Z_i$ and $Z_R = 0$ due to the different $g_{\alpha R}$ and effective fields (5) and (6), respectively. The MFD here decays exponentially for charged radiators, but for a neutral radiator very similar to the Holtsmark MFD, which falls like $E^{-2.5}$.

4. Conclusions and outlook

A similar excellent agreement between the PMFEX treatment and the MD simulations, as shown here, was also found for a wide range of plasma parameters, both for charged and neutral radiators. For the case of a charged radiator further examples, together with a detailed discussion of the limits of the PMFEX treatment at increasing coupling, are given in [12]. Altogether, we thus conclude that the proposed PMFEX treatment is a very reliable method for calculating the MFD of a moderately coupled TCP with attractive interaction, both for charged and neutral radiators.

A natural next step is now to study how these results on the MFD are related to the spectral line profiles in a TCP. Here of course the different timescales for the interaction of the ions and electrons with the perturbed radiator are essential, and the resulting Stark broadening thus strongly depends on the actual conditions. We are currently investigating spectral line shapes by extending the line of development of [14] using the time dependent microfields of strongly coupled TCPs as provided by MD simulations. Some first, preliminary results are given in [15].

Acknowledgments

This work was supported by the Bundesministerium für Bildung und Forschung (BMBF, 06ER128) and by the Gesellschaft für Schwerionenforschung (GSI, ER/TOE).

References

[1] Griem H R 1974 *Spectral Line Broadening by Plasmas* (New York: Academic)
[2] Salzmann D 1998 *Atomic Physics in Hot Plasmas* (Oxford: Oxford University Press)
[3] Holtsmark J 1919 *Ann. Phys., Lpz.* **58** 577
Margenau H 1932 *Phys. Rev.* **40** 387
[4] Baranger M and Mozer B 1959 *Phys. Rev.* **115** 521
Mozer B and Baranger M 1960 *Phys. Rev.* **118** 626
[5] Hooper C F Jr 1966 *Phys. Rev.* **149** 77
Hooper C F Jr 1968 *Phys. Rev.* **165** 215
[6] Iglesias C A 1983 *Phys. Rev.* A **27** 2705
[7] Iglesias C A, Lebowitz J L and MacGowan D 1983 *Phys. Rev.* A **28** 1667
[8] Alastuey A, Iglesias C A, Lebowitz J L and Levesque D 1984 *Phys. Rev.* A **30** 2537
[9] Talin B, Calisti A and Dufty J 2002 *Phys. Rev.* E **65** 056406
[10] Yan X-Z and Ichimaru S 1986 *Phys. Rev.* A **34** 2167
[11] Ortner J, Valuev I and Ebeling W 2000 *Contrib. Plasma Phys.* **40** 555
[12] Nersisyan H B, Toepffer C and Zwicknagel G 2005 *Phys. Rev.* E **72** 036403
[13] Deutsch C, Furutani Y and Gombert M M 1981 *Phys. Rep.* **69** 85
[14] Marten J and Toepffer C 2004 *Eur. Phys. J.* D **29** 397
[15] Nersisyan H B, Toepffer C and Zwicknagel G 2005 *GSI Plasma Annual Report 2004* p 45